

# An Experimental Study on Energy and Exergy for Glazed and Unglazed Solar System with Perforated Absorber Plate and Wire Mesh Layers

Afaq Jasim Mahmood \*

\* Department of Power Mechanics Techniques, Institute of Technology Baghdad, Middle Technical University, Baghdad, Iraq  
(afaqjasem@yahoo.com)

‡ Afaq Jasim Mahmood;, Tel: +964770067560,  
Fax: +964770067560, Dr.Afaq\_jasem100@mtu.edu.iq

*Received: 27.09.2019 Accepted:05.11.2019*

**Abstract-** The purpose of this experimental study is to construct and evaluation three solar heaters (glassed heater 90° bed angle, unglazed heaters 90° bed angle and glassed heater 47° bed angle), these heaters device 50 mm height of the bed with a perforated absorber plate and wire mesh layers. The perforated plate and six steel wire mesh layers were painted black then placed parallel to each other in heater bed; the mesh layers had a cross-sectional area of 2.2 mm× 2.2 mm and an internal diameter of 4.11 mm, perforated plate had an internal hole diameter of 2 mm, pitch 4 mm. In this search, the outlet temperature and thermal efficiency were studied in a geographical zone, located in the Baghdad city, Iraq. The experimental results showed that the thermal efficiency increases as the air velocity increases in the range of 7.5 m/Sec to 2 m/Sec. The maximum thermal efficiency obtained using the glazed solar heater 90° bed slope was 63%, but for unglazed solar heater same bed slops the maximum thermal efficiency decreased to 43.3%. The maximum thermal efficiency increased to 65.6% as decrease the bed slops to the 47° for the glazed heater at a flowing air velocity of 7.5 m/Sec. Additionally, the temperature differences, (the differences between outlet temperature and inlet temperature) and exergy efficiency for three beds of solar heater indicated an inverse association with flowing air velocity: Temperature differences and exergy efficiency, increased as the air velocity decreased. The maximum temperature differences and exergy efficiency for glazed solar heater bed slope 90° were 37.9 °C and 4.8 %, for unglazed solar heater bed slope 90°, temperature differences were 16.8 °C and exergy efficiency was 2.23 %, for glazed solar heater bed slope 47°, The temperature differences and exergy efficiency were 48 °C and 5.24 %, which were recorded for the duration 12:00 am at maximum solar intensity. The results validated an improvement in thermal efficiency, exergy efficiency, and the outlet air temperature.

**Keywords** Unglazed Solar heater, Glazed Solar heater, Thermal efficiency, Exergtic efficiency, Perforated absorber plate.

## 1. Introduction

Energy is vital to human life, most energy is being produced from non-renewable sources, such as fossil fuels, missions from the combustion process have been linked to phenomena such as global warming, acid rain, and photochemical smog. Policymakers and researchers are searching for cost-effective technologies, to reduce energy consumption and CO<sub>2</sub> emissions [1-3]. Using alternative and energy-efficient knowledge's with improved building construction will assistance reduce the heat required for internal heating and thus reduce emissions and resource consumption. Using renewable energy to heat air, for

example the use of solar heater systems, is an effective technique to minimize CO<sub>2</sub> emissions and resource consumption. A conventional solar heater, mainly consists of a rectangular panel, named solar collector, made of materials or wood, an absorber plate puts interior the collector, the top of the collector was covered by a transparent plastic or glass panel, and air blower installation at the end of the collector. All the sides of the solar heating system are thermally isolated, except the upper cover [4-6]. Multiple factors effect on solar heater, the most important parameters effect on the solar system, absorber plate and cover type, which effect on the outlet air temperature and thermal performance. Different configurations can be applied to increase the heat transfer

coefficient of the airflow, perforated absorber plates and a wire mesh layer can be used to increase the absorbing surface area of the absorber plate, while also increasing turbulence inside the flow channel. Glass cover is used to improve the thermal performance of a solar heater because it minimizes the thermal energy lost from the perforated plate to an environment [7].

All sides of the solar heater must be thermally well-insulated, to minimize the convection and radiation heat losses, to the environment. Two researchers S. Chamoli and N. Thakur [8] have investigated a mathematical model, to study the performance of solar collectors with V down perforated baffles as roughness on the air flow side of the absorber plate, a mathematical model was done, to study the effects of surrounding temperature, designed and operated conditions, on thermal efficiency and effective efficiency.

A glazed cover is used with either, a single or double airflow pass, for increasing the coefficient of the heat transfer, for working fluid, which passing between the glass cover, and absorbing plate [9].

The solar heaters use a transparent material [14], [18] or glass panel [11-13], to trap the solar energy inside the collector and decrease the heat losses to the surroundings. The paper for A. Mahmood et al. [10], present using wire mesh as a porous media without absorber plate, the wire mesh layers were placed between the back bed and glass cover. The purpose of their study is to improve the output temperature, and solar heater efficiency, also the results indicated that a maximum solar efficiency done with a maximum air flow rate.

The researcher R. Nowzari et al. [14], was studied an experimental project, to improve the efficiencies for a solar air heater, they were found that the efficiencies of collector with glazed cover are more efficient than the collectors used half or quarter perforated cover made of Plexiglas.

The investigator Farhan and Sahi [15] were experimentally worked, for improving the thermal efficiency, of the solar collectors, with the perforated absorber plate. The experimental results informed that, the absorber perforated plate with high porosity, or with a large number of small holes was more effective, than the perforated plate with less number holes and similar area. It has been clear, that the porosity of perforated plate depended on the pitch value of holes, so the previous researchers, Decker et al. [16], K. Gawlik, C. Kutscher [17], and S. Motahar, A. Alemrajabi [18] had reduced the pitch scale, to improve the thermal efficiency.

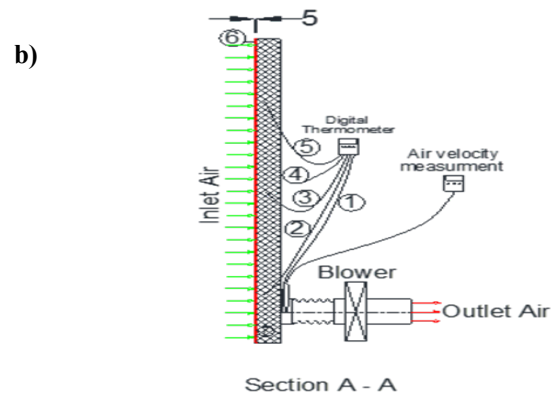
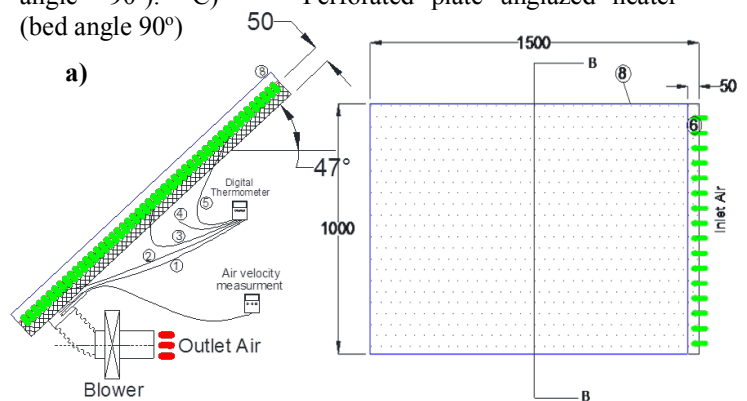
The aim of this manuscript is studying the effect of increasing the absorber plate porosity by inserting porous media inside the plenum channel of glazed and unglazed transpired collectors between perforated plate and back of the bed, the package mesh and perforated plate are acting as an integrated absorption unit. The wire mesh layers used in this solar unit is similar to the prior research were done by A. Omojaro, L. Aldabbagh [19], M. El-khawajah [20], L. Aldabbagh [21] and, A. Mahmood [22], with a difference in the total number and area of layers in order to the enlarged

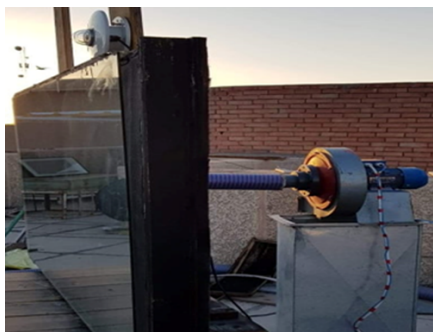
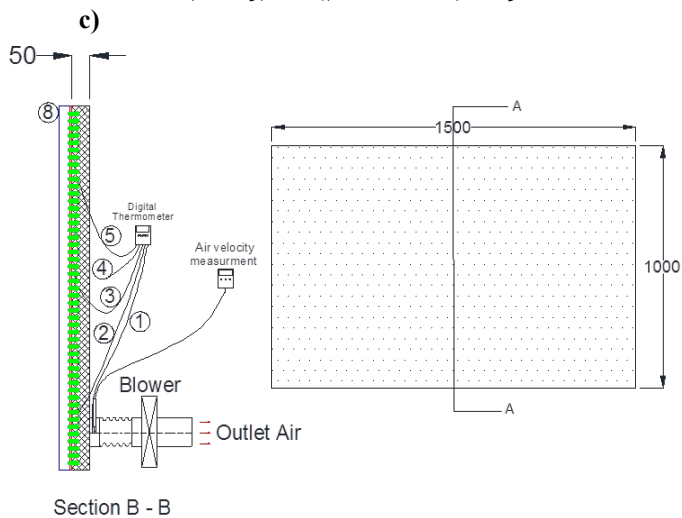
absorber heat region, Experiments are conducted under actual outdoor environments.

**2. Experimental Facility**

*2.1. Experimental Setup*

Three solar heaters were constructed and tested in Baghdad, Iraq (33.3152 °N, 44.3661 °E), the thermal efficiency and exergy efficiency were considered. All collectors were made of wood, rectangular bed sizes of 1.5 m × 1 m, depth of 0.05 m. For improving the solar heater thermal efficiency and exergy efficiency, three beds were colour black to condensate sun emission on them. The practical part of the research is illustrated in Figure1, the photos of the solar heater system, A) Perforated plate glazed heater (bed angle 47°). B) Perforated plate glazed heater (bed angle 90°). C) Perforated plate unglazed heater (bed angle 90°)





1,2,3,4,5) Thermocables (K-Type), 6) Perforated plate.  
 7) Wire mesh layers, 8) Glass cover.

**Fig. 1.** Photos of the solar heater system: **a)** Perforated plate glazed heater (bed angle 47°). **b)** Perforated plate glazed heater (bed angle 90°). **c)** Perforated plate unglazed heater (bed angle 90°).

An outdoor experimental setup was developed to test solar heaters (glazed solar heater system bed angle 47°, glazed solar heater system bed angle 90°, and unglazed solar heater system bed angle 90°). The main components in each setup were the perforated absorber plate, six wire mesh layers, and glazed or unglazed cover. For glazed solar heater, glass cover area was (1.45 m × 1 m), thickness of 4 mm was fixed upper the bed parallel to the perforated absorber plate. There was a rectangular hole on the left side with an area of (1 × 0.05) m<sup>2</sup> to act as the airflow entry. The distance from the glass cover, to the perforated plate was 30 mm, the perforated plate material was galvanized steel, hole diameter 2 mm and pitch 4 mm, perforated plate area (1.5 m × 1 m). Six wire mesh layers with square voids area (2.2 × 2.2) mm<sup>2</sup>, porosity  $\Phi = 0.88$ , absorptivity of 0.96 were located under and parallel to perforated plate (galvanized steel). The distance between the first layer and perforated plate was 3 cm. The wire mesh layers separated between layer to another layer by small pieces of wood to make space high by 0.5 cm, thus the heat transfer from the wire mesh layers, to flowing air were increased. All mesh layers and perforated plate were set equivalent to the glass cover. All mesh layers painted black. In this manner, an elevation of air velocity through holes of perforated plate that increase the heat transfer

coefficient of air and improving the efficiency, then the air moving through mesh layers gain more heat as it passed through the heater bed (mesh layer absorb heat from a perforated plate by radiation than transfer heat to air flow by convection). For unglazed solar heater, the interior air was flowing inside the bed through the holes of the perforated absorber plate, and then touching the wire mesh layers, for this moving period the air absorbing the heat from perforated plate and wire mesh layers. The speed meter was calibrated and used for measuring the air velocity. Small plastic straw tubes 4.7 mm diameter, 30 mm length installed 100 mm after air exits, uniform flow was created; the speed meter was installed in this region. A 0.75 kW blower was connected to the end of the left side heater bed. The blower was controlled by the speed control, named inverter model: 0.01- 400Hz, 5A, SV008iC5-1. Five air speeds reading from 2 to 7.5 m/s were done. The Hot Wire Anemometer (60-90) mA, HT-9829) was calibrated and installed between the outlet duct (end of the bed) and centrifugal fan to measure the air speed. Table 1 presents the operating parameters and design.

## 2.2. Experimental Procedure

The ambient temperature (inlet temperature),  $T_{in}$  was documented by digital thermometer, which was put underneath the solar heated bed. A calibration test set an accuracy of  $\pm 0.5$  °C. Four T-type thermocouples were located in three points in the solar heated bed. A calibration test set an accuracy of  $\pm (0.5^\circ\text{C}, +0.4\%)$ . The first three thermocouples were used to measure the heater bed temperature  $T_{bed}$  ( $T_{bed1}$ ,  $T_{bed2}$  and  $T_{bed3}$ ). The forth thermocouple was used to measure the outlet air temperature  $T_{out}$  and was attached inside the wire mesh. All the temperatures were measured by using (EXTECH), 4-channel thermometer, model SDL200, an accuracy of  $\pm (0.4\% + 0.5^\circ\text{C})$ . Hourly solar intensity was registered from a Pyranometer that was placed up and close to the solar heater collector. Hourly wind speed and humidity data were taken from the Iraqi meteorological organization and seismology. Inlet temperature, solar intensity, bed temperature, outlet temperature, wind speed and humidity were recorded from 8:00 am to 5:00 pm for five day equivalent to five air velocity from 2-7.5 m/Sec. The solar heaters, with steady-state conditions were done; the air was circulated for 30 min prior to the period in which the data were taken.

## 3. Energy and Exergy Analysis

### 3.1 Energy Analysis

The performance of a solar heater can be measured in terms of the collector thermal efficiency; thermal efficiency can be stated as the ratio of the amount of the useful energy gain to the amount of the incident solar radiation [23].

$$\eta = \frac{m C_p (T_o - T_i)}{I A_c} \quad (1)$$

Thermal efficiency [24], also was solved by experimental equation from another concept, which was used the heat removal factor ( $F_R$ ) as given:

**Table 1.** The basic design used for the experimental study.

Parameter	Value
Solar Heater Location	Baghdad- Iraq
Solar Heater Slope	47° degree: Is the angle, where the sun's rays are concentrated on the surface of the solar collector, to reach the maximum absorption of solar energy, (33 °N and 44 °E)
Solar Heater Orientation	South
Experiment date	March 2019
Solar Heater Length	1.5 m
Solar Heater Width	1 m
Solar Heater Depths	0.05 m
Perforated Absorber	Diameter of 2 mm, Pitch 4 mm
Wire Mesh Layers	6 layers, porosity Φ= 0.88, absorptivity of 0.96
Glass Thickness	4 mm
Centrifugal Fan	0.75 kW, Model 135C16A
Pyranometer	RK200-03, SN:R18021068, Range: 0-2000 W/m <sup>2</sup> .

$$\eta = F_R \left[ (\tau\alpha) - (U_L) \frac{(T - T_a)}{I} \right] \tag{2}$$

The parameter that effect on the heat removal factor of the heater system (F<sub>R</sub>) is the outlet air temperature, so the heat removal factor can be calculated by Hottel–Whillier–Bliss equation:

$$F_R = \frac{mC_p(T_o - T_i)}{A_c [I(\tau\alpha) - U_L(T - T_a)]} \tag{3}$$

### 3.2 Exergy Analysis

Second law of thermodynamics was applied to express the exergy efficiency for solar heater collectors, exergy efficiency defined as a relation of absorbed exergy (EX<sub>u</sub>) for passing air to the amount of exergetic sun radiation (EX<sub>in</sub>) that depend on sun temperature and environment temperature on the collector [25]. Exergy efficiency analysis is the best way for researchers to reach the optimal design for solar heating system.

$$\eta_{Ex} = \frac{EX_u}{EX_{in}} = 1 - \frac{EX_{dest}}{EX_{in}} \tag{4}$$

Exergy destruction (EX<sub>dest</sub>) is defined as the amount of input exergy subtracted from exergy of the sun radiation:

$$EX_{dest} = EX_{in} - EX_u \tag{5}$$

The exergy of sun radiation (input exergy) [20] is defined as:

$$EX_{in} = \left( 1 + \frac{1}{3} \left( \frac{T_a}{T_{sun}} \right)^4 - \frac{4T_a}{3T_{sun}} \right) I . A_c \tag{6}$$

The exergy that absorbed by passing air of the solar system was calculated from the equation (7):

$$EX_u = m \left[ C_p(T_o - T_i) - T_a \left( C_v \ln \left( \frac{T_o}{T_i} \right) - R \ln \left( \frac{\rho_{out}}{\rho_{in}} \right) \right) \right] \tag{7}$$

T<sub>a</sub> refers to the ambient temperature (inlet temperature was same value of ambient temperature), and 5600 (K) is the solar intensity temperature, T<sub>sun</sub>, [26].

### 4. Uncertainty Analysis

An error related to the practical measurements was gained after performing the experimental work. The uncertainty analysis of the thermal efficiency is obtainable in this part. However, Holmans method was applied for calculating the uncertainty of the thermal efficiencies [27]. In general, the (ω<sub>x</sub>) is the uncertainty of X, it can be defined as:

$$\omega_x = \left[ \left( \frac{\partial x}{\partial y_1} \omega_{y_1} \right)^2 + \left( \frac{\partial x}{\partial y_2} \omega_{y_2} \right)^2 + \dots + \left( \frac{\partial x}{\partial y_n} \omega_{y_n} \right)^2 \right]^{1/2} \tag{8}$$

Where; y<sub>1</sub>, y<sub>2</sub>, . . . , y<sub>n</sub> are parameters associated with the variance of X.

The solar heater efficiency can be formulated as the following:

$$\eta = \frac{Q}{I.A_c} = \frac{\rho \cdot \dot{V} \cdot c_p \cdot \Delta T}{I.A_c} \tag{9}$$

Where;

$$\Delta T = T_{out} - T_{in} = T_{out} - T_a \tag{10}$$

$$Q = \dot{m} \cdot c_p \cdot \Delta T = \rho \cdot \dot{V} \cdot c_p \cdot \Delta T \tag{11}$$

$$\dot{V} = v \cdot (0.25 \cdot \pi \cdot d_{out}^2) \tag{12}$$

If equation (9) is substituted in equation (8), the uncertainty of solar heater efficiency is arranged as the equation below:

$$\omega\eta = \left[ \left( \frac{\dot{V}c_p\Delta T}{AI} \omega\rho \right)^2 + \left( \frac{\rho c_p \Delta T}{AI} \omega\dot{V} \right)^2 + \left( \frac{\rho\dot{V}\Delta T}{AI} \omega c_p \right)^2 + \left( \frac{\rho\dot{V}c_p}{AI} \omega\Delta T \right)^2 + \left( -\frac{\rho\dot{V}c_p\Delta T}{A^2I} \omega A \right)^2 + \left( \frac{\rho\dot{V}c_p\Delta T}{AI^2} \omega I \right)^2 \right]^{\frac{1}{2}} \tag{13}$$

Following Eq. (8), the total uncertainty in heat output ( $\omega Q$ ) and volumetric flow rate ( $\omega V$ ) can be written as an equation [20- 21] & [27]:

$$\omega Q = \left[ (\dot{V} c_p \Delta T \omega \rho)^2 + (\rho c_p \Delta T \omega \dot{V})^2 + (\rho \dot{V} \Delta T \omega c_p)^2 + (\rho \dot{V} c_p \omega \Delta T)^2 \right]^{\frac{1}{2}} \tag{14}$$

$$\omega_v = \left[ (0.25 \cdot \pi \cdot d_{out}^2 \cdot \omega_v)^2 + (0.5 \cdot v \cdot \pi \cdot d_{out} \cdot \omega_d)^2 \right]^{1/2} \tag{15}$$

Assuming ( $C_p$ ) specific heat, ( $\rho$ ) density and, ( $A$ ) area of the solar heater are constant in a field of work temperatures, the uncertainty of solar heating system efficiency is associated with  $V$ ,  $\Delta T$ , and  $I$ . The average values of the results are calculated and the volumetric air flow rates are determined for each working day to obtain the uncertainties.

**Table 2.** The uncertainty for calculations and measurements.

Solar heater type	Perforated plate glazed heater (bed angle 90°)	Perforated plate unglazed heater (bed angle 90°)	Perforated plate glazed heater (bed angle 47°)
$\omega\eta$ %	±0.41	±0.37	±0.87
$\omega Q$ (W)	±11.44	±9.78	±11.64
$\omega V$ (m <sup>3</sup> /hr)	±1.21	±0.87	±1.41
$\omega \rho$ (kg/m <sup>3</sup> )	0	0	0
$\omega C_p$ (KJ/kg.K)	0	0	0
$\omega \Delta T$ (°C)	±0.5	±0.5	±0.5
$\omega A$ (m <sup>2</sup> )	±0.002	±0.002	±0.002
$\omega L$ & $\omega w$ (mm)	±0.5	±0.5	±0.5
$\omega I$ (W/m <sup>2</sup> )	±7	±7	±7
$\omega D$ (mm)	±0.5	±0.5	±0.5
$\omega v$ (m/Sec)	±0.01	±0.01	±0.01

For the perforated plate unglazed heater (bed angle 90°), the average of total results for all of the variables  $V$ ,  $I$ ,  $\Delta T$ ,  $T_{in}$ ,  $T_{out}$ ,  $T_{air}$ , and wind speed, air humidity, were calculated to be: 7.68 °C, 29.70 °C, 37.38 °C, 33.54 °C, 0.49 m<sup>3</sup>/Sec, 717.2 W/m<sup>2</sup>, 13.1 km/hr, 24.3%. The uncertainty of volumetric flow rate ±0.87 m<sup>3</sup>/h ( $\omega V$ ), the uncertainty of gain energy ( $\omega Q$ ) ±9.78 W, the uncertainty of thermal efficiency ±0.366 %.

For perforated plate glazed heater (bed angle 90°), the average of total results for all of the variables  $V$ ,  $I$ ,  $\Delta T$ ,  $T_{in}$ ,  $T_{out}$ , and wind speed, air humidity, were calculated to be: 17 °C, 22.9 °C, 40.9 °C, 31.9 °C, 0.49 m<sup>3</sup>/Sec, 602.2 W/m<sup>2</sup>, 14.14 km/ hr, 34.7%. The uncertainty of volumetric flow rate ±1.21 m<sup>3</sup>/h ( $\omega V$ ), the uncertainty of gain energy ( $\omega Q$ ) ±11.44 W, the uncertainty of thermal efficiency ±0.412%.

For perforated plate glazed heater (bed angle 47°), the average of total results for all of the variables  $V$ ,  $I$ ,  $\Delta T$ ,  $T_{in}$ ,  $T_{out}$ ,  $T_{air}$  and wind speed, air humidity, were calculated to be: 26.86 °C, 57.87 °C, 42.28 °C, 0.49 m<sup>3</sup>/Sec, 660 W/m<sup>2</sup>, 19.2 km/hr, 40.9 %. The uncertainty of volumetric flow rate ±1.41 m<sup>3</sup>/h ( $\omega V$ ), the uncertainty of gain energy ( $\omega Q$ ) ±11.64 W, the uncertainty of thermal efficiency ±0.872%. The uncertainty of the above equations results is listed in Table 2. Values for density and specific heat are taken from the documents of Z. Bonca et al. [28].

### 5. Results and discussion

By using the commercial software Engineering Equation Solver (EES), exergy and energy efficiency are studied analytically, for three solar thermal systems, these solar heaters have similar characteristics, with single-flow collector, perforated absorber plate, and a packed bed in place of six wire mesh layers, behind perforated plate to increase the absorbing area, the differences between these three solar system are: 1. Perforated plate glazed solar heater (bed angle 90°), 2. Perforated plate glazed heater (bed angle 90°), 3. Perforated plate unglazed heater (bed angle 47°), all these heaters was structured at 33.3152 °N, 44.3661 °E in a

climate conditions of the Baghdad, capital of Iraq during April 2019, April was a dry month, clear blue sky with an average maximum temperature 29.0°C and 258 hours of the sun.

5-1 Energy Analysis

5-1-1 Perforated Plate Glazed Heater (bed angle 90°)

The inlet temperature and hourly variation of the measured solar intensity for perforated absorber plate glazed heater (bed angle 90°) are described in Figures 2 and 3, for the range of air velocity between (2- 7.5) m/Sec. As shown in Figure 2, the inlet temperature versus time of the day was prepared, the inlet temperature versus time of the day curves seem the same behaviour, with similar shape graphs for all day of the experiments. The inlet temperature directly depended on weather factors such as wind velocity, solar intensity, air humidity, because of clear sky on April, all inlet temperature curves reached their maximum values at afternoon from 14.00 to 15.00 pm, with similar shape graph for all day of the experiments. The maximum average degree for temperature 24.4 °C, wind speed 14.14 km/hr and relative humidity 40 %. The average inlet temperature degree at 8.00 am equal 17.4 °C, but at the end of the days (17.00 pm) was 24 °C, although the solar intensity was decreased to minimum value. The reason of this phenomena, because the environment loses heat slowly.

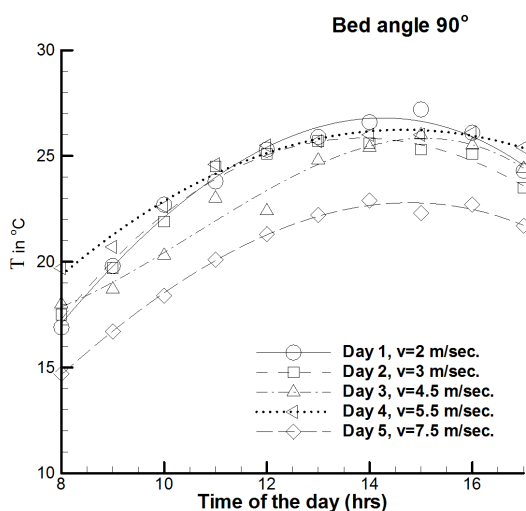


Fig. 2. Inlet temperature against time of a day for glazed heater (bed angle 90°).

Solar intensity, I, data set were registered for five sunny days constantly from 8.00 am to 17.00 pm (Figure 2), were shown as five curves, a little variation of the solar intensity curves, the values of solar intensity of each curve were close to each other, therefore the accurate process results were done. All curves reach a peak value at 12:00 am (the solar radiation incident was perpendicular to the bed angle of 90° at time 12:00), then slowly decreased until sunset to the minimum value at 17.00 pm. The maximum value (860 w/m<sup>2</sup>) of solar intensity, its at a maximum air velocity (7.5 m/Sec).

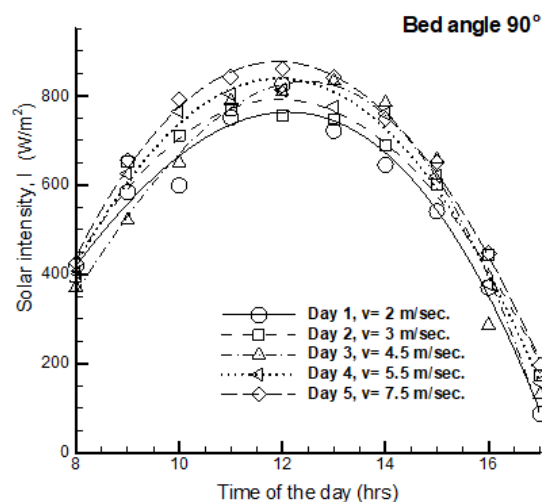


Fig. 3. Solar intensity against time of a day for glazed heater (bed angle 90°).

The relation between the temperature difference, ΔT, (outlet temperature- inlet temperatures) with time of day for air velocities in the range of (2- 7.5) m/Sec are indicated in Figure 4, bed angle 90°. The temperature difference ΔT, observed a similar arrangement for all of the days of the experiments, The temperature difference ΔT, was increased from morning until midday between 12:00 and 1:00 pm, at which point it reached the maximum value, and then slowly decreased until sunset (given a shape same as the solar intensity graph). The maximum value of ΔT was 37.9 °C for maximum solar intensity 825 W/m<sup>2</sup> and lower air velocity of 2 m/Sec. The graph clearly shows that ΔT decreased as the air velocity increased. Decreasing the air velocity reduced the time of passing air through the bed heater, which increased the heat transfer between perforated plate and wire mesh layers with flowing air by convection, thus the outlet temperature and ΔT were increased.

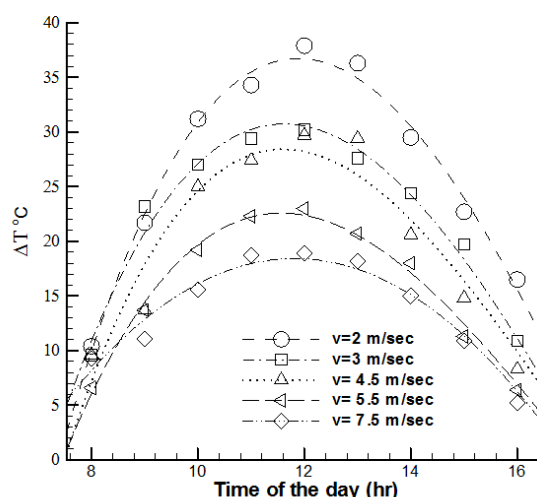
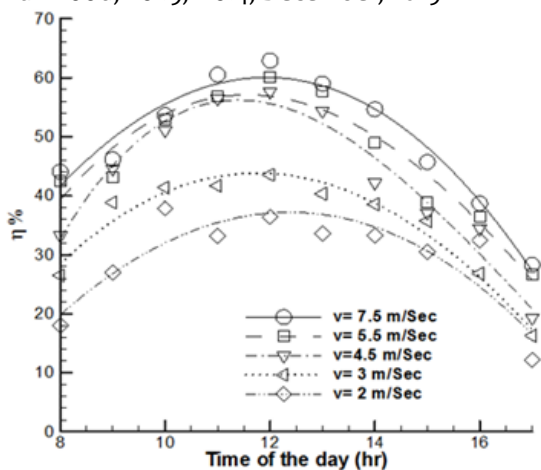


Fig. 4. Temperature difference against time of a day at different air velocity for glazed heater (bed angle 90°).

The Solar heater efficiency with time of a day are presented in a Figure 5 for different air velocity from (2 to 7.5) m/Sec.



**Fig. 5.** Variation of thermal efficiency of different air velocity for glazed heater (bed angle 90°).

The efficiency constantly increasing with the air velocity increase. The behaviour of heat transfer coefficient of air is correlated with air velocity, when the air velocity increased, the convective heat transfer coefficient was increased, thus the heat transfer from the heater to the working fluid was improved. The 63% was a maximum efficiency gained at an air velocity of 7.5 m/Sec. It is clear from the Figure 5, maximum points of the thermal efficiency curves were at 12:00 am, after 12:00 am the efficiencies curves were gradually decreasing till evening at 5:00 p.m., these curves similar behaviours to the temperature difference,  $\Delta T$  and the solar intensity, curves. The increase in the solar intensity increased the outlet temperature and thermal efficiency.

**5.1.2 Perforated Plate Unglazed Heater (bed angle 90°)**

The solar intensity, temperature differences, and inlet air temperatures, versus time of day for bed angle 90°: (a) Air velocity 2 m/Sec, (b) Air velocity 7.5 m/Sec was prepared in Figure 6. The exergy efficiency,  $\eta_{Ex}$ , values were being determined by solar intensity, outlet and inlet air temperatures, from 8:00 am to 5:00 pm, for two air flow velocities, minimum velocity 2 m/Sec, and maximum air velocity 7.5 m/Sec, for perforated plate unglazed heater (bed angle 90°). Outlet and inlet air temperatures, associations with solar intensity are presented the same performance curves, for velocity 2 m/Sec, and velocity 7.5 m/Sec. The maximum solar intensity 936 W/m<sup>2</sup>, for air velocity 2 m/Sec. As shown in Figure 6, the maximum solar intensity 967 W/m<sup>2</sup>, for air velocity 7.5 m/Sec, therefore the maximum temperature differences,  $\Delta T$  equal 16.8 °C for air velocity 2 m/Sec and 15 °C for air velocity 7.5 m/Sec.

The Solar heater efficiencies, with time of a day are presented in a Figure 7, at 2 m/Sec, and 7.5 m/Sec air velocity. The efficiencies continuously are increased, when the air velocity increased, (i.e. The useful gain energy was directly proportional to the air velocity), The high efficiencies attained for air velocity 2 m/Sec, 7.5 m/s were 12.1% and 43.3%, respectively. It was clear from Figure 6, that the efficiency at 7.5 m/Sec higher than in air velocity 2 m/Sec, this is due to, the energy was gained from the sun's heat, and, that energy was absorbed from the mesh layers, and perforated plate.

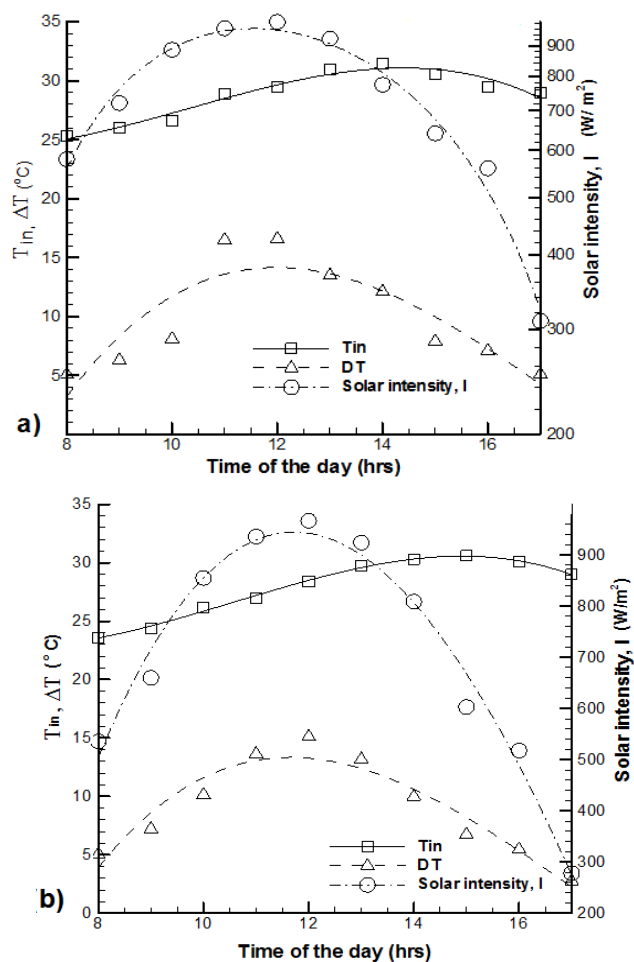


**Fig. 6.** Solar intensity, inlet air temperatures and temperature differences against time of day for: a) Air velocity 2 m/Sec, b) Air velocity 7.5 m/Sec.

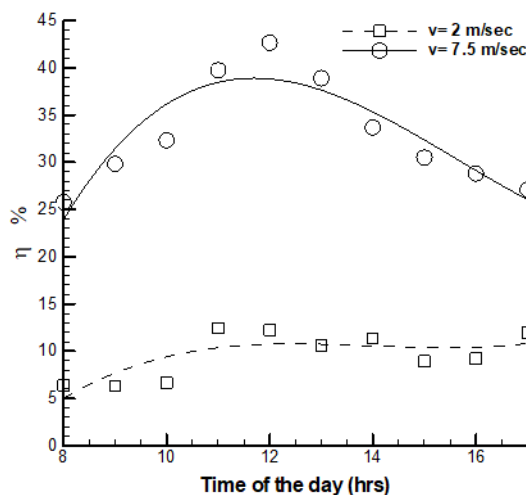


**Fig. 7.** Variation of thermal efficiencies at different air flow velocities for perforated plate unglazed heater (bed angle 90°): a) Air velocity 2 m/Sec, b) Air velocity 7.5 m/Sec.

**5.1.3 Perforated Plate Glazed Heater (bed angle 47°)**

Third collector for this research was tilted 47°, for maximized the sun radiation falling on collector area,

(absorbing maximum radiation), thus, the heat radiation transferred, from the sun, to the perforated absorber plate, and mesh layers, then to the working fluid were enhancements. To reduce the heat lost from the perforated absorbing plate, the glass cover was done, therefor the collector with perforated plate glazed heater (bed angle 47°) was more efficient than others (as shown above), the maximum efficiency,  $\eta$ , 65.61%, for 7.5 m/Sec at solar intensity,  $I$ , 926 W/m<sup>2</sup>, inlet temperature,  $T_{in}$ , 29 °C and  $\Delta T$ , 48 °C temperature differences, (Figure 8 and Figure 9).

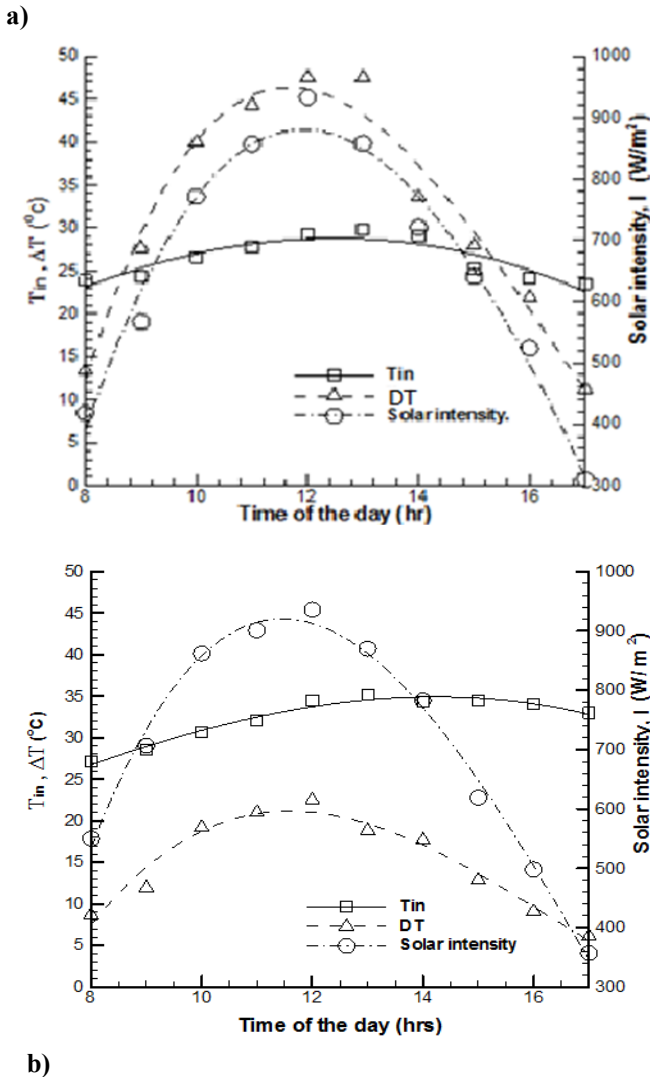


**Fig. 8.** Inlet air temperatures, temperature differences and solar intensity against time of day: a) Air velocity 2 m/Sec, b) Air velocity 7.5 m/Sec.

5.2 Exergy Analysis

The disadvantage of all solar heater systems was that the heat was transferred from cover solar heater bed to the surrounding, this attracted the attention of researchers to reach an optimal state for balancing between the amount of heat lost outside collector and heat absorbed inside the solar collector from the sun, thus exergy consideration by applying the second law of thermodynamics was appropriate.

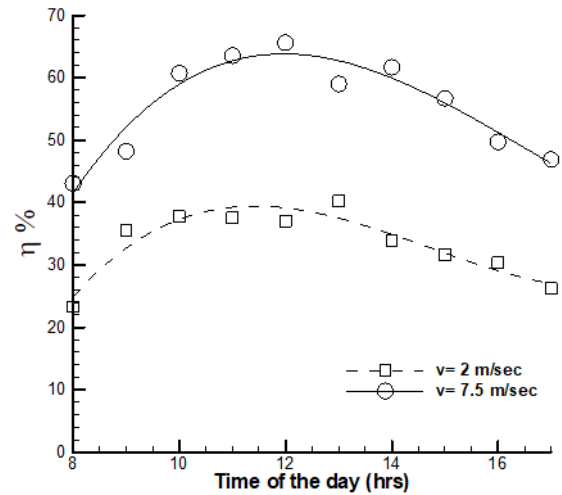


**Fig. 9.** Variation of thermal efficiencies at different air flow velocities for perforated plate glazed heater (bed angle 47°): a) Air velocity 2 m/Sec, b) Air velocity 7.5 m/Sec.

5.2.1 Perforated Plate Glazed Heater (bed angle 90°)

The value of the exergic efficiencies, versus different air velocity, was done as presents Figure 10. The exergic efficiencies for all air velocities from 2 to 7.5 m/Sec were increased from morning at 8.00 am to reach maximum value at 12.00 pm (follow the path line of the solar intensity graph). Furthermore, exergy efficiency ( $\eta_{Ex}$ ) was increased as air velocity decreased, therefore the high value of exergy efficiency  $\eta_{Ex} = 4.8\%$  was recorded at air velocity 2 m/Sec, that mean a high exergy loss of heat, from the absorber perforated plate to surrounding from the time, when the air velocity increased. But at low air velocity, the outlet temperature, and exergy heat gain were increased, which leads increased exergy efficiency.

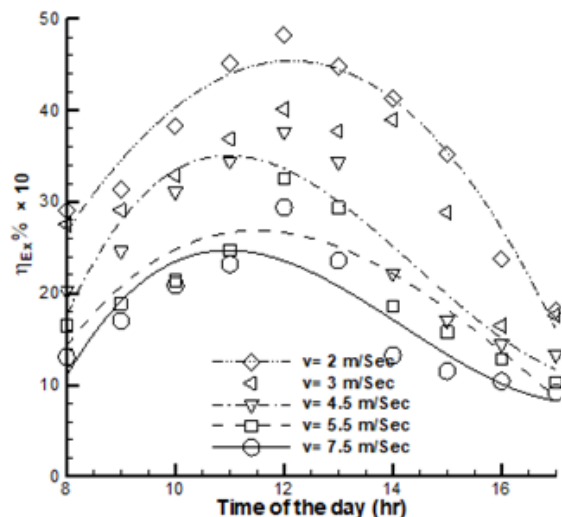


**Fig. 10.** Presents the exergy efficiencies versus different air velocity for glazed heater (bed angle 90°).

5.2.2 Perforated Plate unglazed heater (bed angle 90°)

The exergy efficiency of unglazed solar heater system was less than exergic efficient for glazed heater, cause more heat gone into the environment from the absorber plate, as



shown in Figure 11, the maximum efficiency was  $\eta_{Ex} = 2.23\%$ .

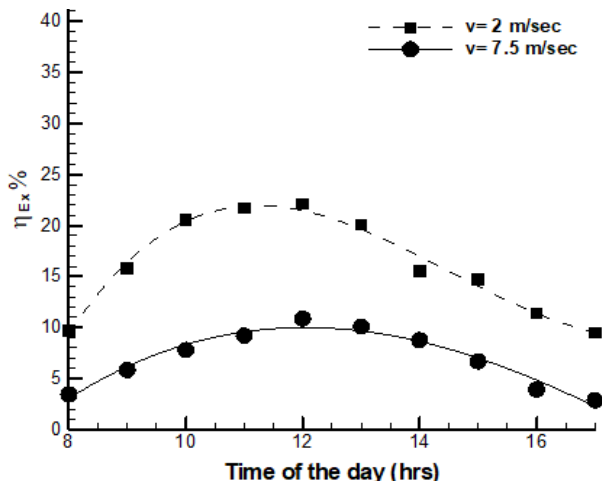


**Fig. 11.** Presents the exergy efficiencies versus different air velocity for perforated plate unglazed heater (bed angle 90°).

5.2.3 Perforated Plate Glazed Heater (bed angle 47°)

As present in Figure 12, the exergy efficiencies with time of the day from 8 am to 5 pm for 7.5 and 2 m/Sec, the curves increased from morning (8.00 am) to reach the maximum value at noon (12.00 pm), then decrease at the end of the work (5.00 pm), the exergy efficiencies constantly increasing with the air velocity decrease. The collector tilted to 47° there was an enhancement of exergy efficiency when compared with collector tilted to 90°, to reach the maximum value,  $\eta_{Ex} = 5.24 \%$  at a minimum air velocity 2 m/Sec. As the air velocity increased the exergy efficiencies were decreased.

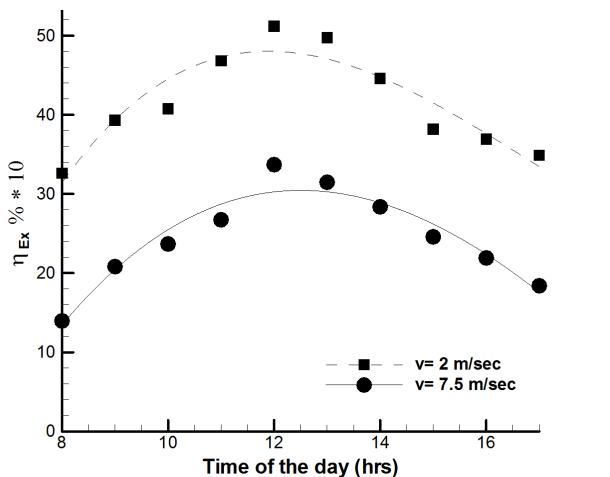


**Fig. 12.** Presents the exergy efficiencies versus different air velocity perforated plate glazed heater (bed angle 47°)

6. Conclusion

The glazed and unglazed solar heater with perforated absorber plate and wire mesh layers were constructed and tested for different air velocity from 7.5 m/Sec to 2 m/Sec and different angle bed 90° and 47°. The effect of inlet air temperature, air velocity, temperature difference and solar

radiation, on exergy efficiency, and thermal efficiency was indicated. The practical results of the proposed design indicate that the exergy efficiency, and the thermal efficiency, of the glazed solar heater system were better than unglazed solar heater system, for same air velocity, also was obtained that the exergy efficiency, and the thermal efficiency, for solar heater angle of 47° was more efficient, than solar heater of 90°, for equivalent air velocity. Thermal efficiency will increase by increasing the air velocity, but the exergy efficiency was found to be reduced with increasing the air velocity. For both glazed and unglazed solar heater system, the temperature difference between the outlet air temperature and inlet air temperature decreased as the air velocity increased, for the glazed solar heater, bed angle of 47°, the temperature difference was greater than that of glazed and unglazed solar heater bed angle of 90°.

NOMENCLATURE

$A=A_c$	Absorbed area (m <sup>2</sup> )
$C_p$	Specific heat of air (kJ/kg.K)
$EX_{dest}$	Exergy of the destruction (W)
$EX_{in}$	Inlet exergy (W)
$E_{xu}$	Exergy useful (W)
$F_R$	Solar removal factor
$I$	Solar intensity (W/m <sup>2</sup> )
$m$	Mass flow rate (kg/s)
$Q$	Energy gain (W)
$T_{air}$	$(T_{in}+T_{out}) / 2$ (°C)
$T_a$	Temperature of surrounding (°C)
$T_i$	Temperature of inlet air (°C)
$T_{sun}$	Sun Temperature (K)
$T_{out}$	Temperature of outlet air (°C)
$\Delta T$	Temperature difference ( $T_o-T_i$ )
$U_L$	Overall heat loss coefficient (W/m <sup>2</sup> . °C).
$\dot{V}$	Volumetric flow rate (m <sup>3</sup> /Sec)
$\rho$	Air density (kg/m <sup>3</sup> )
$\Phi$	Porosity
$\tau\alpha$	Transmissivity- absorptivity
$\eta$	Thermal efficiency
$\eta_{Ex}$	Exergy efficiency

References

[1] S. Kalogirou, "Solar thermal collectors and applications", Progress in Energy and Combustion Science, vol. 30, pp. 231- 295, February 2004.

- [2] K. Ishikawa, S. Obara, M. Takabatake, R. Kawai, "Investigation of the Heat Cycle of a CO<sub>2</sub> Hydrate Using Plate Type Heat Exchangers", 4th International Conference on Renewable Energy Research and Applications, Palermo, Italy, 22-25 November 2015.
- [3] K. Kajiwara, K. Tsuji, S. Ikeda, N. Matsui, F. Kurokawa, "Performance Mechanism of Active Clamp Resonant SEPIC Converter in Renewable Energy Systems", 4th International Conference on Renewable Energy Research and Applications, Palermo, Italy, 22-25 November 2015.
- [4] R. Atia, N. Yamada, "Distributed Renewable Generation and Storage Systems Sizing in Deregulated Energy Markets", 4th International Conference on Renewable Energy Research and Applications, Palermo, Italy, 22-25 November 2015.
- [5] E. Kabalci, Y. Kabalci, R. Canbaz, G. Gokkus, "Single Phase Multilevel String Inverter for Solar Applications" 4th International Conference on Renewable Energy Research and Applications, Palermo, Italy, 22-25 November 2015.
- [6] A. Mahmood, "Exergy Analysis of flat plate Solar Air heaters Having Obstacles and Filled with wire Mesh Layers", 2nd International Conference on Sustainable Engineering Techniques, Baghdad, Iraq, pp. 032001-10, 6-7 March 2019.
- [7] S. Aboul-Enein, A. El-Sebaii, M. Ramadan and H. El-Gohary, "Parametric study of a solar air heater with and without thermal storage for solar drying applications" *Renewable Energy*, vol. 21, pp. 505- 522, November 2000.
- [8] S. Chamoli and N. Thakur, "Performance study of solar air heater duct having absorber plate with V down perforated baffles", *Songklanakarin J. Sci. Technol.* Vol. 36, pp. 201-208, December 2014.
- [9] S. Kalogirou, "Design, construction, performance evaluation and economic analysis of an integrated collector storage system", *Renewable Energy*, Vol. 12, pp. 179-192, October 1997.
- [10] A. Mahmood, L. Aldabbagh, F. Egelioglu, "Investigation of single and double pass solar air heater with transverse fins and a package wire mesh layer", *Energy Conversion and Management*, vol. 89, pp. 599-607, October 2015.
- [11] A. Mohamad, "High efficiency solar air heater", *Solar Energy* vol. 60, pp. 71-76, October 1996.
- [12] A. El-abidi, S. Yadir, F. Chanaa, M. Benhmida, H. Amiry, H. Bousseta, H. Ezzaki, "Modeling and Simulation of a Modified Solar Air Heater Destined to Drying the *Gelidium Sesquipedale*", *International Journal of Renewable Energy Research*, vol.8, 2003-2014.
- [13] V. Ermuratskii, V. Oleschuk, F. Blaabjerg, "Experimental Investigation of Two Modified Energy - Saving Constructions of Solar Greenhouses", 4th International Conference on Renewable Energy Research and Applications, Palermo, Italy, 22-25 November 2015.
- [14] R. Nowzari, L. Aldabbagh and F. Egelioglu, "Single and double pass solar air heaters with partially perforated cover and packed mesh". *Energy*, vol. 73, pp. 694-702, 2014.
- [15] A. Farhan and H. Sahi, "Energy Analysis of Solar Collector With perforated Absorber Plate", *Journal of Engineering*, Vol. 23, pp. 89-102, September 2017.
- [16] G. Decker, K. Hollands and A. brunger, "Heat-exchange relations for unglazed transpired solar collectors with circular holes on a square or triangular pitch", *Solar Energy*, vol. 71, pp. 33-45, 2001.
- [17] K. Gawlik and C. Kutscher, "Wind Heat Loss from Corrugated, Transpired Solar Collectors" *Transactions of the ASME*, Vol. 124, pp. 256-261, 2002.
- [18] S. Motahar and A. Alemrajabi, "An Analysis of Unglazed Transpired Solar Collectors Based on Exergetic Performance Criteria", *Int. J. of Thermodynamics*, vol. 13, pp. 153-160, 2010.
- [19] A. Omojaro, L. Aldabbagh, "Experimental performance of single and double pass solar air heater with fins and steel wire mesh as absorber", *Apply Energy*, vol. 87, pp. 3759-3765, 2010.
- [20] M. El-khawajah, L. Aldabbagh and F. Egelioglu, "The effect of using transverse fins on a double pass flow solar air heater using wire mesh as an absorber" *Sol Energy*, vol. 85, pp. 1479-87, 2011.
- [21] L. Aldabbagh, F. Egelioglu and M. Ilkan, "Single and double pass solar air heaters with wire mesh as packing bed", *Energy*, vol. 35, pp. 3783-3787, 2010.
- [22] A. Mahmood, "Experimental Study of a Solar Air Heater With A New Arrangement of Transverse Longitudinal Baffles", *Journal of Solar Energy Engineering*, vol. 139, pp. 031004-1- 031004-12, JUNE 2017.
- [23] H. Ajam, S. Farahat and F. Sarhaddi, "Exergetic Optimization of Solar Air Heaters and Comparison with Energy Analysis", *Int. J. of Thermodynamics*, vol. 8, pp. 183-190, December 2005.
- [24] C. Malvi, A. Gupta, M. Gaur, R. Crook and D. Dixon-Hardy, "Experimental investigation of heat removal factor in solar flat plate collector for various flow configurations", *International Journal of Green Energy*, vol. 14, pp. 442-448, 2017.
- [25] F. Bayraka, H. Oztop and A. Hepbasli, "Energy and exergy analyses of porous baffles inserted solar air heaters for building applications". *Energy and Buildings*, vol. 57, pp. 338-345, 2013.
- [26] H. Esen, " Experimental Energy and Exergy Analysis of A Double-Flow Solar Air Heater Having Different

Obstacles On Absorber Plates", Building and Environment, vol. 43, pp. 1046–1054, 2008

- [27] J. P. Holman, Experimental Methods for Engineers, 8th ed., vol. 13. McGraw-Hill Series in Mechanical Engineering, 2011, pp. 36-72.
- [28] Z. Bonca, D. Butrymowicz, T. Hajduk and w. Targański, New coolants and heat medi-ums 1st ed., Thermal and performance properties [in Polish], IPPU MASTA, Gdańsk 2004, pp. 45-86.